Desalination and Water Treatment
www.deswater.com

doi: 10.1080/19443994.2013.782256

52 (2014) 199–207
January

Taylor & Francis
Taylor & Francis Group

Synthesis of glutamic acid-modified magnetic corn straw: equilibrium and kinetic studies on methylene blue adsorption

Ying Zhao[1], Yunxue Xia[1], Hongyu Yang, Yanyan Wang, Maojun Zhao*

Deparment of Chemistry, College of Life and Science, Sichuan Agricultural University, Yaan 625014, P.R. China
Tel. +86 835 8563240; Fax: +86 835 2862227; email: zmjun01@yahoo.com.cn

Received 29 January 2013; Accepted 26 February 2013

ABSTRACT

Magnetic corn straw (MCS) was prepared by glutaraldehyde cross-linking, and the resulting MCS was chemically modified with glutamic acid to synthesize glutamic acid-modified MCS (GMCS). GMCS was investigated by scanning electron microscopy, Fourier-transform infrared spectroscopy, and potentiometric titration. The results reveal that nano-Fe_3O_4 was stably cross-linked with the corn straw, and the carboxyl on the MCS surface was modified. GMCS was used for the adsorption of methylene blue (MB). Several factors affecting MB adsorption on MCS and GMCS, namely, pH, contact time, initial MB concentration, and reaction temperature were investigated. The adsorption capability of GMCS for MB was observed to be superior to that of MCS. The maximum adsorption capacity of GMCS for MB (196.46 mg g^{-1}) was attained with an initial MB concentration of 300 mg L^{-1} at pH 6.0 and 60°C for a contact time of 60 min. The adsorption process followed the pseudo-second-order kinetic model and the Langmuir isotherm equation. Desorption and regeneration experiments were conducted, and the recovery efficiencies were maintained between 90 and 70% using absolute ethanol as eluent.

Keywords: Corn straw; Magnetic; Glutamic acid; Adsorption; Methylene blue

1. Introduction

Given the outstanding industrial development, large amounts of dyes are widely used in textiles, cosmetics, paper, leather, pharmaceuticals, food, and other industries. However, waste water from dye production can lead to various environmental problems. Among the various dyes, methylene blue (MB) is a typical cationic dye that is mainly used in textiles [1–3], which is difficult to remove from the environment because of its complex aromatic ring structure. Thus, the development of an effective method to remove MB from the environment is urgently needed. In recent years, the adsorption method has been highly valued because of its effectiveness, low cost, easy availability, and ability to treat dyes in more concentrated forms [4–6]. Numerous absorbent materials have been successfully used to remove dyes from waste water [7–9]. However, poor absorption capacity and regeneration have limited their practical applications. The problem of regeneration can efficiently be solved by the magnetic separation technique [10,11].

*Corresponding author.

[1]*Ying Zhao and Yunxue Xia are equal for the first author.*

Corn waste, a cost-effective, easily available, and safe biological material, has shown great potential for the removal of dyes and heavy metals [12,13]. Corncobs, as corn waste, are mainly applied for the absorption of heavy metals and dyes in waste water [14,15]. Several studies have reported that untreated corn straw (CS) waste has low adsorptive capacity, which cannot meet the technical requirement of modern industry. Therefore, modifying CS waste is necessary. According to previous reports, the amount and species of functional groups, such as hydroxyls and carboxyls, on the surface of adsorbents are significantly responsible for their adsorption capacity in waste water treatment [16–20]. In this work, glutamic–acid was used to modify magnetic corn straw (MCS) to prepare glutamic acid-modified magnetic corn straw (GMCS). GMCS was characterized by scanning electron microscopy (SEM), Fourier-transform infrared spectroscopy (FTIR), and potentiometric titration analyses. GMCS was used to adsorb MB, and the adsorption mechanism was also examined.

2. Materials and methods

2.1. MB solutions

MB was purchased from Tianjin Chemical Reagent No. 1 Plant, China. A stock solution of MB was prepared by dissolving 1.0 g of MB in 1 L of deionized water. Various working concentrations (50–450 $mg\,L^{-1}$) were obtained by diluting the stock solution. The pH of the solution was adjusted to the desired level by adding a small quantity of HCl ($0.1\,mol\,L^{-1}$) or NaOH ($0.1\,mol\,L^{-1}$).

2.2. CS pretreatment

CS was washed with deionized water several times to remove soluble impurities and adhered dirt. The sample was dried, crushed, and screened through a set of sieves with geometrical particle sizes of 100 mesh. The resulting sample was dispersed in NaOH ($0.1\,mol\,L^{-1}$) at 60°C for 2 h and washed with deionized water until pH 7.0 was reached. Finally, the dried sample was stored in an airer for further use.

2.3. MCS preparation

Magnetic nano-Fe_3O_4 was preformed according to a previous report [21]. CS (10.0 g) was stirred in 200 mL of glutaraldehyde solution (0.5 wt% in water) for 12 h, and, then nano-Fe_3O_4 (2.0 g) was added to the suspension. After continuous shaking for another 24 h at room temperature, MCS was magnetically separated by an applied magnetic field. Finally, the MCS product was washed several times to remove the remaining glutaraldehyde and dried under vacuum at 60°C [22].

2.4. GMCS preparation

Glutamic acid (2.0 g) was added to 150 mL of deionized water and adjusted to pH 10 in a conical flask, and then 5.0 g of MCS was added. The mixture was stirred at room temperature for 24 h to yield GMCS. The GMCS obtained was separated from the mixture by an external magnet and was washed several times with deionized water. Finally, GMCS was freeze-dried under high vacuum for 24 h and was preserved in a desiccator for further use.

2.5. Adsorption studies

Batch adsorption studies were conducted in 250 mL conical flasks at different temperatures (15, 30, 45, 60, and 80°C). Each adsorbent (0.05 g) was added to 50.0 mL of MB solution at initial concentrations of 50–450 $mg\,L^{-1}$. The suspension was agitated at 200 $r\,m^{-1}$ by a rotary shaker (DH2−DA, China) for the required adsorption time (10–120 min) and different pH values. The desired initial solution pH (3.0–9.0) was obtained by adjusting with $0.1\,mol\,L^{-1}$ HCl or $0.1\,mol\,L^{-1}$ NaOH. Then, the mixture was magnetically separated, and the supernatant fractions were evaluated to determine the residual MB concentration by spectrophotometry (WFJ-7200 Spectrophotometer, China) at λ_{max} of 640 nm. The adsorption capacity was measured by the following relationship:

$$Q_t = (C_i - C_t)V/m \quad (1)$$

where Q_t ($mg\,g^{-1}$) is the amount of adsorption capacity at time t; C_i and C_t are the initial and equilibrium concentrations of MB ($mg\,L^{-1}$), respectively; V is the volume of the solution (L); and m is the mass of the related biosorbent (g).

2.6. Regeneration studies

MCS (0.05 g) and GMCS (0.05 g) were added into 50.00 mL of 300 $mg\,L^{-1}$ MB solution at room temperature. The MB-loaded adsorbent was magnetically separated and rinsed thrice with deionized water. Then, the adsorbent that settled was eluted with absolute ethanol. The mixture was harvested by magnetic separation, and the supernatant was analyzed. The MCS/GMCS regeneration and MB recovery efficiency were calculated by the following relationships:

$$\text{Recovery efficiency} = \frac{\text{Amount of dye desorbed}}{\text{Amount of dye adsorbed}} \times 100 \quad (2)$$

$$\text{Regeneration efficiency} = \frac{\text{Regeneration adsorption capacity}}{\text{Original adsorption capacity}} \times 100 \quad (3)$$

2.7. MCS and GMCS characterization

The surface structure and morphology of MCS and GMCS were characterized using SEM (JEOL JSM-5900LV, Japan) at a 20 kV acceleration voltage. Prior to analysis, the samples were coated with a thin gold layer.

The binding group types present on MCS and GMCS were identified using FTIR (Shimadzu FTIR-8400s, Japan) within the region 400–4,000 cm^{-1} via the KBr pressed-disk method. The active sites present on the surface of MCS and GMCS were determined by potentiometric titration using an autotitrator (ZD-2, China) with a combined glass electrode. Data analysis was performed using the non-electrostatic model of the software Protofit Version 2.0 [23–26]. This useful software tool for the calculation of pKa values and surface site densities of biological materials was used to fit the acid–base titration data of the MCS and GMCS.

3. Results and discussion

3.1. Effect of pH on adsorption

Fig. 1 shows the adsorption capacity of the two adsorbents for MB at pH 3.0–9.0. With increasing pH, the MB adsorption capacity of MCS and GMCS increased, and the maximum uptakes of MB (87.56 mg g^{-1} for MCS and 172.14 mg g^{-1} for GMCS) were observed at pH 6.0. At low pH, several protons are available to protonate the adsorbent surface. Thus, the electrostatic repulsion between the positively charged adsorption sites and the positively charged MB ions results in poor adsorption capacity [27,28]. As the pH increases, the adsorbent surface becomes more negatively charged, and the functional groups (such as carboxyl, amino, and hydroxyl groups) are more deprotonated. Thus, the electrostatic attraction force of the positively charged MB ions with the adsorbent surface likely increased. At pH > 6.0, the adsorption capacity nearly remained constant with increasing pH. This effect can be attributed to the reduced electrostatic attraction force between the adsorbent and MB. Thus, the optimum pH for MB adsorption of GMCS was found at pH 6.0, and GMCS showed a higher adsorption capacity for MB compared with MCS. Carboxyl groups exhibit a determining function on the adsorption process. Abundant adsorption sites were produced in GMCS because of the glutamic acid-rich MCS surface, which resulted in its higher adsorption capacity for MB. Although various functional groups, such as carboxyl, amine, and hydroxyl, were present on the MCS surface, their amount for adsorption was limited [29]. Thus, the adsorption capacity of GMCS was greater than that of MCS.

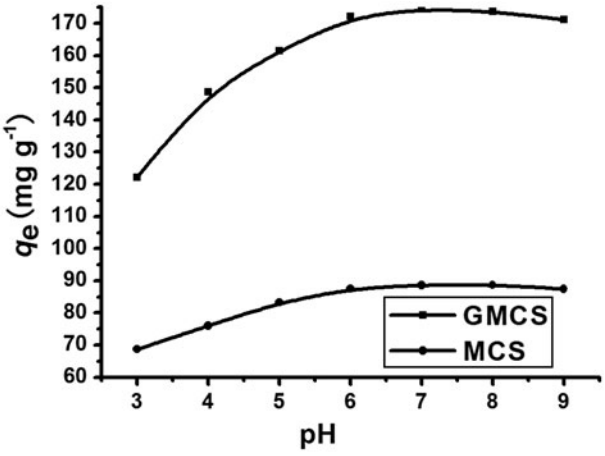

Fig. 1. Effect of pH on MB biosorption.

3.2. Effect of contact time and kinetics analysis

The effect of different contact times (10–120 min) on the adsorption process with constant initial dye concentration of 300 mg L^{-1}, solution pH 6.0, and room temperature was examined. Fig. 2 presents the MB adsorption kinetics of MCS and GMCS. The contact time curve shows that the dye was rapidly adsorbed by the two adsorbents during the first 30 min. As time passed, the adsorption capacity increased, and the adsorption equilibrium time was 60 min. MB molecules gradually penetrated into the porous adsorbents and were slowly adsorbed by the functional groups in the internal cell wall for further physical adsorption. In addition, the amount of carboxyl groups increased due to the introduction of glutamic acid. Thus, the MB adsorption capacity of GMCS was higher than that of MCS. Finally, the optimum contact time was selected as 60 min for further adsorption experiments.

To analyze the MB adsorption kinetics of MCS and GMCS, the pseudo-first-order and

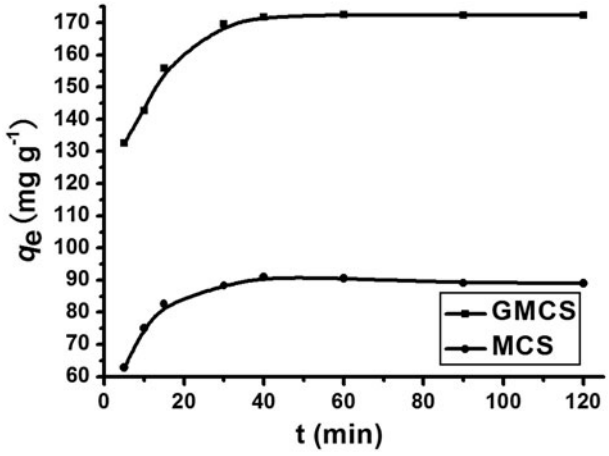

Fig. 2. Effect of contact time on MB biosorption.

pseudo-second-order kinetic models were tested using the experimental data. The pseudo-first-order kinetic model and the pseudo-second-order kinetic model are given in the following forms [30,31]:

$$\text{Pseudo-first-order equation: } \ln(q_e - q_t) = -k_1 t + \ln q_e \quad (4)$$

$$\text{Pseudo-second-order equation: } \frac{t}{q_t} = \frac{1}{k_2 q_e^2} + \frac{t}{q_e} \quad (5)$$

where q_e and q_t (mg g^{-1}) are the adsorption capacity values at equilibrium and time t, respectively; k_1 is the rate constant of the pseudo-first-order equation (min^{-1}); k_1 is the slope of the linear plot of ln (q_e−q_t) versus t; and k_2 is the rate constant of the pseudo-second-order equation (g mg^{-1} min^{-1}). The slopes of the linear plot of t/q_t versus t represent k_2.

As shown in Table 1, the correlation coefficient values (R^2) of the pseudo-second-order kinetics are greater than that of the pseudo-first-order kinetics. The calculated values of adsorption capacity ($q_{e,\text{cal}}$) for pseudo-second-order kinetics were more approximate to the experimental values ($q_{e,\text{exp}}$), indicating the better applicability of the pseudo-second-order kinetics model. The results suggest that the adsorption process involved chemisorption and physisorption. Chemisorption is the rate-determining step, where valence forces are involved because of electron sharing or exchange between the functional groups on the adsorbents and the MB ions [32]. The linear plots of t/q_t versus t are shown in Fig. 3.

3.3. Effect of initial MB concentration and adsorption isotherms

The MB adsorption isotherms of MCS and GMCS at room temperature and pH 6.0 are shown in Fig. 4. The results show that the MB adsorption capacity of MCS and GMCS increased rapidly with increasing initial MB concentration. This result is attributed to the increased collision efficiency between the dye molecules and the adsorbents with the increase in initial MB concentration in solution. However, MB adsorption capacity remained almost constant at higher initial MB concentrations. This result is due to the lack of sufficient binding sites to accommodate more MB ions at higher concentration levels [33].

The experimental data were modeled with Langmuir and Freundlich isotherms. The Langmuir adsorption isotherm explains the adsorption of basic dyes from aqueous solutions, whereas the Freundlich isotherm is appropriate to describe multilayer adsorption with interactions between adsorbed molecules. The linear forms of the Langmuir and Freundlich models are expressed as follows:

$$\text{Langmuir model: } \frac{C_e}{q_e} = \frac{C_e}{q_m} + \frac{1}{bq_m} \quad (6)$$

$$\text{Freundlich model: } \ln q_e = \frac{1}{n}\ln C_e + \ln K_F \quad (7)$$

where q_e and q_m are the equilibrium and maximum adsorption capacities (mg g^{-1}), respectively; C_e is the equilibrium MB concentration in solution (mg L^{-1}); b (L mg^{-1}) is the Langmuir adsorption equilibrium constant; K_F (L mg^{-1}) is the Freundlich adsorption constant; and $1/n$ is the heterogeneity factor.

Table 1
Comparison of the pseudo-first-order and the pseudo-second-order adsorption rate constants and the calculated and experimental q_e values

Biosorbents	$q_{e\ \text{exp}}$ (mg g^{-1})	Pseudo-first-order kinetic model			Pseudo-second-order kinetic model		
		k_1 (min^{-1})	R^2	$q_{e\ \text{cal}}$ (mg g^{-1})	k_2 (g mg^{-1}min^{-1})	R^2	$q_{e\ \text{cal}}$ (mg g^{-1})
MCS	85.97	0.0322	0.7706	13.36	0.008163	0.9994	86.96
GMCS	172.46	0.0677	0.8892	37.20	0.003612	0.9998	175.44

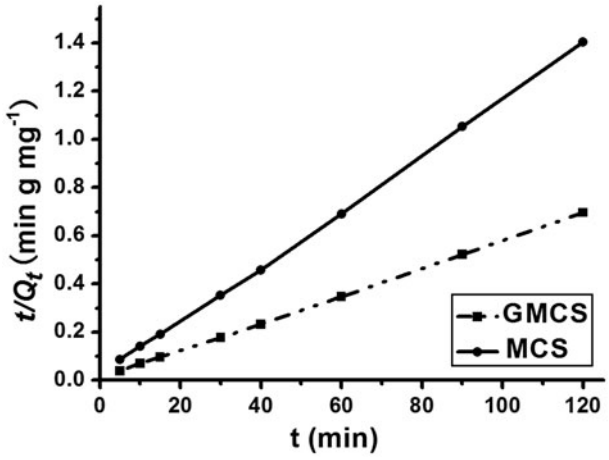

Fig. 3. Pseudo-second-order kinetic isotherms of MCS and GMCS.

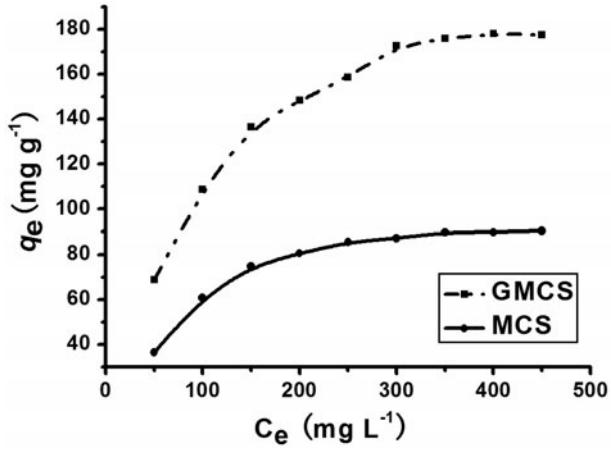

Fig. 4. Effect of initial MB concentration.

Table 2
Langmuir and Freundlich isotherm constants and correlation coefficients for adsorption

Biosorbents	Langmuir constant				Freundlich constant		
	q_m (mg g^{-1})	b (L mg^{-1})	R^2	R_L	$1/n$	k_F	R^2
MCS	108.7	0.0127	0.9953	0.4189	0.39	9.328	0.8903
GMCS	222.2	0.009785	0.9976	0.1851	0.4356	14.63	0.9425

As shown in Table 2, the experimental data showed a better fit with the Langmuir isotherm for MB adsorption based on the correlation coefficients (R^2). This result revealed that the process was based on monolayer adsorption that mostly occurred on the surface-active areas of MCS and GMCS. The Langmuir isotherm linear plots for MB adsorption are shown in Fig. 5.

To determine whether the adsorption was ''favorable'' or ''unfavorable,'' a dimensionless constant separation factor or equilibrium parameter, R_L, was calculated using the following equation:

$$R_L = \frac{1}{1 + bC_m} \tag{8}$$

where C_m is the highest initial MB concentration (mg L^{-1}), and R_L indicates the type of isotherm as irreversible ($R_L = 0$), favorable ($0 < R_L < 1$), linear ($R_L = 1$), or unfavorable ($R_L > 1$) [34].

The values of R_L were found to be 0.4189 for MCS and 0.1851 for GMCS, indicating that the MB adsorption of MCS and GMCS was favorable. The MB adsorption of GMCS was more favorable compared with that of MCS.

3.4. Effect of temperature

The effect of temperature on the equilibrium adsorption capacity of MCS and GMCS for MB (300 mg L^{-1}, pH 6.0) was investigated in the temperature range 15–80°C. As shown in Fig. 6, the adsorption capacity increased simultaneously with the increase in reaction temperature from 15–60°C. The maximum

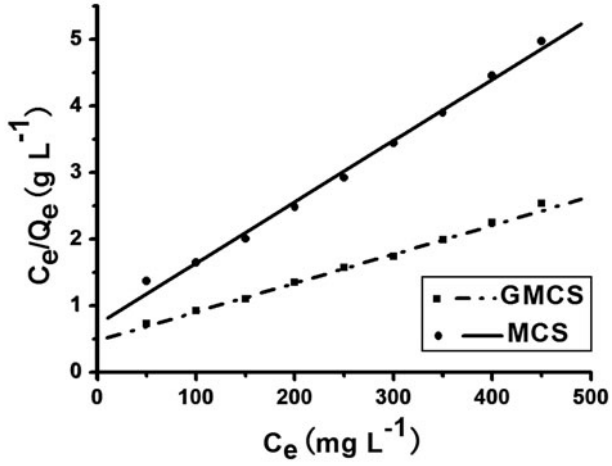

Fig. 5. Langmuir isotherms for MB biosorption of MCS and GMCS.

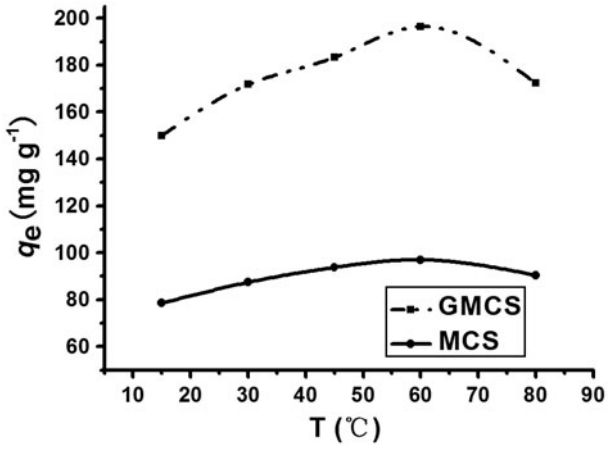

Fig. 6. Effect of temperature.

MB adsorption capacity observed at 60℃ was 96.98 mg g^{-1} for MCS and 196.46 mg g^{-1} for GMCS. These results are attributed to the increased mobility of MB ions with increasing temperature [35,36]. With increasing reaction temperature, the amount of non-protonated functional groups on the two adsorbents increases due to the increase in the dissociation constant of the protonated carboxyl groups. Furthermore, increasing temperature can cause a swelling effect within the internal structure of the two adsorbents. This effect enabled the MB ions to penetrate further, resulting in enhanced adsorption capacity. Nevertheless, the adsorption capacity decreased significantly when the temperature exceeded 60℃. This result is due to the major force (i.e. electrostatic interactions) involved in dye ion binding, which might be weakened because of increasing temperature from the exothermic electrostatic interactions [37]. As the hydrolysis degree of the ester bond increases with increasing reaction temperature, several carboxyl groups could separate from the adsorbent surface via hydrolysis [38]. Thus, the adsorption capacity of MB decreased rapidly at temperatures above 60℃.

3.5. Regeneration studies

MB adsorption/desorption cycles were repeated four times using absolute ethanol. The results obtained are given in Table 3. The regeneration and recovery efficiency of GMCS were maintained between 90 and 70%. The decrease in regeneration efficiency with increasing adsorption/desorption cycles was due to irreversible adsorption and MB loss in the process of reuse. Table 3 shows that GMCS is a stable recyclable adsorbent.

4. Characterization

4.1. SEM analysis

The surface structures of nano-Fe_3O_4, CS, and GMCS were analyzed by SEM, and the results are given in Fig. 7. Fig. 7(a) shows that the nano-Fe_3O_4 particles were uniform, scattered, and fine. The average particle diameter was approximately 200 nm. Fig. 7(b) shows the tubular structure of CS, and its surface appeared to be loose and smooth. Fig. 7(c) illustrates the rather rough, shriveled, and irregular GMCS surface. This structure is attributed to the nano-Fe_3O_4 that adhered on baker's yeast surface and to the glutaraldehyde treatment, which cross-linked some biomass surfaces. The large number of granular materials found on the surfaces of GMCS was due to nano-Fe_3O_4 that adhered on the CS surface. During the preparation of GMCS, vacuum freeze-drying resulted in a highly porous biomass form with a very large surface area. Thus, the permeability of GMCS was improved via sublimation and dehydration, which is beneficial for adsorption and recovery.

4.2. Determination of active sites

Functional groups on the MCS and GMCS surface were determined by potentiometric titration. By combining the microorganism cell wall structure and the

Table 3
Results of biosorption and desorption

	Adsorbents			
	MCS		GMCS	
A/D cycle	Uptake (mg g^{-1})	MB recovery efficiency (%)	Uptake (mg g^{-1})	MB recovery efficiency (%)
1	77.63	89.99	154.17	90.37
2	75.334	87.34	149.98	87.93
3	67.53	78.28	135.04	79.16
4	58.65	67.98	117.4	68.82

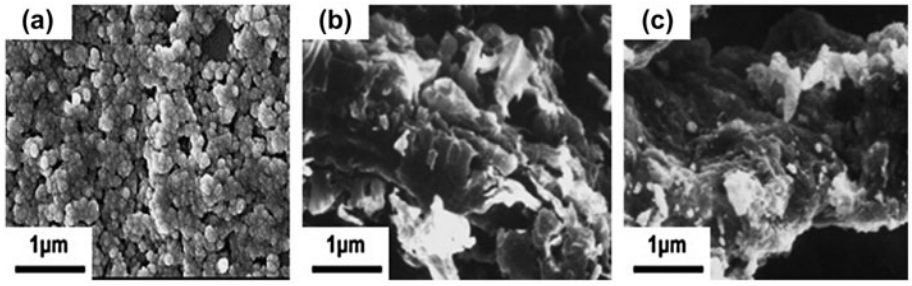

Fig. 7. SEM micrographs of nano-Fe_3O_4 (a), CS (b), and GMCS (c).

Table 4
Concentration and acidity constants of the surface functional groups on MCS and GMCS

Functional group	pKa value reported	MCS		GMCS	
		pKa value obtained	Site density (mmol g^{-1})	pKa value obtained	Site density (mmol g^{-1})
Carboxyl	2.0–6.0	2.23	0.95 ± 0.04	5.82	1.74 ± 0.01
Phosphoryl	0.2–2.9	7.03	1.06 ± 0.07	5.21	0.81 ± 0.04
	5.6–7.2				
Amine	9.0–11.0	10.51	0.52 ± 0.02	9.06	0.58 ± 0.03
Hydroxyl	8.0–12.0	11.32	1.83 ± 0.08	11.82	0.81 ± 0.05

IR results of MCS and GMCS, the functional groups mainly present on the surface of MCS and GMCS were found to be carboxyl, amino, hydroxyl, and phosphoryl groups. The acidity constant values (pKa) and site concentrations for each type of surface functional group were calculated by Protofit Version 2.0, and the results are shown in Table 4. The total concentration of carboxyl and phosphoryl groups on GMCS is significantly higher than that on MCS, and the amino group density on GMCS is almost the same as MCS. Thus, the glutaraldehyde modification increased the amount of carboxyl groups on GMCS. With the repeated vacuum freeze-drying during the preparation of GMCS, the outer structure layer of the cell wall was destroyed and the inner protein layer (carboxyl and phosphoryl groups) was more exposed. Thus, more exposed intracellular phosphoryl and carboxyl groups were detected on the surface of GMCS. By contrast, as shown in Table 4, the amount of hydroxyl on GMCS is significantly lower than that on MCS.

4.3. IR analysis

The IR spectra for CS, MCS, and GMCS are shown in Fig. 8. As shown in Fig. 8, the spectrum for pristine CS was simple. Absorbance peaks were observed at 3,336, 2,900, 1,558, and 1,057 cm^{-1} (Fig. 8(c). The broad strong peak at 3,336 cm^{-1} corresponds with the overlapping of –NH/–OH stretching vibration absorbance. The peak at 2,900 cm^{-1} is attributed to the –CH stretching vibration. The peak at 1,558 cm^{-1} indicates C–N from the bending band of N–H from the amide II band functional group. The peaks at 1057.0 cm^{-1} are attributed to the *glycitols* (C–OH) and the stretching band of P–O–C.

After modification with nano-Fe_3O_4 and glutamic acid, several changes in IR spectra were found, as shown in Fig. 8(a) and (b). First, for GMCS, not only did the decrease in the absorption peak strength of

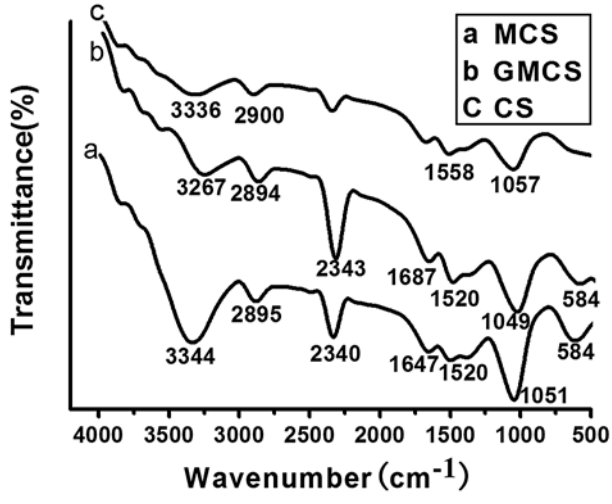

Fig. 8. IR spectra for MCS(a), GMCS (b) and CS (c).

–NH/–OH stretching vibration occur, but the broad overlapping peak also shifted from 3,344–3,267 cm^{-1}. Second, at around 2343 cm^{-1}, the C=O absorbance peak intensity was enhanced. This result means that a large number of carboxyl groups were introduced to the MCS surface via the glutamic acid modification. The –OH band of GMCS also shifted to the lower wave numbers compared with MCS. Furthermore, the significant adsorption peaks around 584 cm^{-1} indicates the characteristic stretching band of Fe–O, confirming that both MCS and GMCS were loaded with nano-Fe_3O_4.

5. Conclusions

GMCS was obtained and characterized in this study. The synthesized GMCS had good adsorption capacity for MB and possessed super-paramagnetic nano-Fe_3O_4 characteristics for isolation and recovery. The adsorption capability of GMCS for MB was superior to that of MCS. The maximum adsorption capacity (196.46 mg g^{-1} for MB) was attained at pH 6.0 with an initial MB concentration of 300 mg L^{-1} at 60˚C for a contact time of 60 min. The kinetics and equilibrium of the process were explained adequately by the pseudo-second-order kinetic model and the Langmuir isotherm, respectively. The results of potentiometric titration and the FTIR data indicate that the glutamic acid modification remarkably increased the quantity of carboxyl groups on GMCS. Regeneration studies confirmed that GMCS can be efficiently recycled for MB removal.

Acknowledgments

This research was supported by the Key Basic Research Program of the Sichuan Provincial Education Commission, PR China (Grant Nos. 10ZB034) and the Basic Research Program of the Science & Technology Department of Sichuan Province, PR China (Grant No. 2011ZR0067). Sincere thanks go to anonymous reviewers for helpful suggestions.

References

[1] M.C. Shih, Kinetics of the batch adsorption of methylene blue from aqueous solutions onto rice husk: effect of acid-modified process and dye concentration, Desalin. Water Treat. 37 (2012) 200–214.
[2] M.S. Sajab, C.H. Chia, S. Zakaria, Citric acid modified kenaf core fibres for removal of methylene blue from aqueous solution, Bioresour. Technol. 102 (2011) 7237–7243.
[3] Y.M. Wang, B.T. Tang, S.F. Zhang, A visible colorimetric pH sensitive chemosensor based on azo dye of benzophenone, Dyes Pigm. 91 (2011) 294–297.
[4] J.M. Abdula, S. Vigneswarana, W.G. Shimb, J. Kandasamya, Removal of metsulfuron methyl by granular activated carbon adsorption, Desalin. Wat. Treat. 21 (2010) 247–254.
[5] D.A. Fungaro, M. Bruno, L.C. Grosche, Adsorption and kinetic studies of methylene blue on zeolite synthesized from fly ash, Desalin. Water Treat. 2 (2009) 231–239.
[6] H. Deng, J.J. Lu, G.X. Li, G.L. Zhang, X.G. Wang, Adsorption of methylene blue on adadsorbent materials produced from cotton stalk, Chem. Eng. J. 172 (2011) 326–334.
[7] O. Anjaneya, M. Santoshkumar, S.N. Anand, T.B. Karegoudar, Biosorption of acid violet dye from aqueous solutions using native biomass of a new isolate of *Penicillium* sp, Int. Biodeterior. Biodegrad. 63 (2009) 782–787.
[8] M.T. Sulak, H.C. Yatmaz, Removal of textile dyes from aqueous solutions with eco-friendly biosorbent, Desalin. Water Treat. 37 (2012) 169–177.
[9] J. Yang, K.Q. Qiu, Preparation of activated carbons from walnut shells via vacuum chemical activation and their application for methylene blue removal, Chem. Eng. J. 165 (2010) 209–217.
[10] Y.F. Shen, J. Tanga, Z.H. Nie, Y.D. Wang, Y. Ren, L. Zuo, Preparation and application of magnetic Fe_3O_4 nanoparticles for waste water purification, Sep. Purif. Technol. 68 (2009) 312–319.
[11] Y.C. Chang, D.H. Chen, Preparation and adsorption properties of monodisperse chitosan-bound Fe_3O_4 magnetic nanoparticles for removal of Cu(II) ions, J. Colloid Interf. Sci. 283 (2005) 446–451.
[12] X.C. Chen, G.C. Chen, L.G. Chen, Y.X. Chen, J. Lehmann, M. B. McBride, A.G. Hay, Adsorption of copper and zinc by biochars produced from pyrolysis of hardwood and corn straw in aqueous solution, Bioresour. Technol. 102 (2011) 8877–8884.
[13] N. Bagheri, J. Abedi, Adsorption of methane on corn cobs based activated carbon, Chem. Eng. Res. Des. 89 (2011) 2038–2043.
[14] G.Q. Tan, H.Y. Yuan, Y. Liu, D. Xiao, Removal of lead from aqueous solution with native and chemically modified corncobs, J. Hazard. Mater. 174 (2010) 740–745.
[15] R. Leyva-Ramos, L.E. Landin-Rodriguez, S. Leyva-Ramos, N.A. Medellin-Castillo, Modification of corncob with citric acid to enhance its capacity for adsorbing cadmium(II) from water solution, Chem. Eng. J. 180 (2012) 113–120.
[16] C.S. Shen, Y. Shen, Y.Z. Wen, H.Y. Wang, W.P. Liu, Fast and highly efficient removal of dyes under alkaline conditions using magnetic chitosan-Fe(III) hydrogel, Water Res. 45 (2011) 5200–5210.
[17] J.X. Yu, M. Tong, X.M. Sun, B.H. Li, Biomass grafted with polyamic acid for enhancement of cadmium(II) and lead(II) adsorptionm, React. Funct. Polym. 67 (2007) 564–572.
[18] Q. Li, Y. Su, Q.Y. Yue, B.Y. Gao, Adsorption of acid dyes onto bentonite modified with polycations: kinetics study and process design to minimize the contact time, Appl. Clay Sci. 53 (2011) 760–765.
[19] R.M. Gong, Y.Z. Sun, J. Chen, H.J. Liu, C. Yang, Effect of chemical modification on dye adsorption capacity of peanut hull, Dyes Pigm. 67 (2005) 175–181.
[20] M.N. Khan, M.F. Wahab, Characterization of chemically modified corncobs and it s application in the removal of metal ions from aqueous solution, J. Hazard. Mater. 141 (2006) 237–244.
[21] Z. Shan, W.S. Yang, X. Zhang, Q.M. Huang, H. Ye, Preparation and characterization of carboxyl-group functionalized superparamagnetic nanoparticles and the potential for bioapplications, J. Braz. Chem. Soc. 18 (2007) 1329–1335.
[22] K.J. Tiemann, G. Gamez, K. Dokken, J.G. Parsons, J.L. Gardea-Torresdey, Chemical modification and X-ray absorption studies for lead(II) binding by Medicago sativa(alfalfa) biomass, Microchem. J. 71 (2002) 287–293.

[23] S.Q. Memon, N. Memon, S.W. Shah, M.Y. Khuhawar, M.I. Bhanger, Sawdust-agreen and economical adsorbent for the removal of cadmium(II) ions, J. Hazard. Mater. 139 (2007) 116–121.
[24] A. Arkleit, H. Moll, G. Bernhard, Interaction of uranium(VI) with lipopolysaccharide, J. Chem. Soc. Dalton Trans. 21 (2008) 2879–2886.
[25] P. Lodeiro, A. Fuentes, R. Herrero, D.E. Sastre, M.E. Vicente, Cr(III) binding by surface polymers in natural biomass: the role of carboxylic groups, Environ. Chem. 5 (2008) 355–365.
[26] B.F. Turner, J.B. Fein, Protofit: a program for determining surface protonation constants from titration data, Comput. Geosci. 32 (2006) 1344–1356.
[27] K. Marungrueng, P. Pavasant, Removal of basic dye (Astrazon Blue FGRL) using macroalga Caulerpa Lentillifera, J. Environ. Manage. 78 (2006) 268–274.
[28] Y.S. Ho, T.H. Chiang, Y.M. Hsueh, Removal of basic dye from aqueous solution using tree fern as a adsorbent, Process Biochem. 40 (2005) 119–124.
[29] V. Padmavathy, Adsorption of nickel(II) ions by baker's yeast: kinetic, thermodynamic and desorption studies, Bioresour. Technol. 99 (2008) 3100–3109.
[30] E.N. El Qada, S.J. Allen, G.M. Walker, Adsorption of methylene blue onto activated carbon produced from steam activated bituminous coal: a study of equilibrium adsorption isotherm, Chem. Eng. J. 124 (2006) 103–110.
[31] L.C. Zheng, Z. Dang, X.Y. Yi, H. Zhang, Equilibrium and kinetic studies of adsorption of Cd(II) from aqueous solution using modified corn stalk, J. Hazard. Mater. 176 (2010) 650–656.
[32] S.R. Shukla, R.S. Pai, Adsorption of Cu(II), Ni(II) and Zn(II) on dye loaded groundnut shells and sawdust, Sep. Purif. Technol. 43(1) (2005) 1–8.
[33] M. Dogan, H. Abak, M. Alkan, Adsorption of methylene blue onto hazelnut shell: kinetics, mechanism and activation parameters, J. Hazard. Mater. 164 (2009) 172–181.
[34] S. Dahiya, R.M. Tripathi, A.G. Hegde, Adsorption of heavy metals and radionuclide from aqueous solutions by pretreated arca shell biomass, J. Hazard. Mater. 150 (2008) 376–386.
[35] T. Robinson, B. Chandran, P. Nigam, Effect of pretreatments of three waste residues, wheat straw, corncobs and barley husks on dye adsorption, Bioresour. Technol. 85(2) (2002) 119–124.
[36] L.C. Morals, O.M. Freitas, E.P. Goncalves, L.T. Vasconcelos, C.G. González Beça, Reactive dyes removal from wastewatets by adsorption eucalyptus bark: variables that defme the process, Water Res. 33(4) (1999) 979–998.
[37] Y.S. Zhang, W.G. Liu, M. Xu, F. Zheng, M.J. Zhao, Study of the mechanisms of Cu^{2+} adsorption by ethanol/caustic-pretreated baker's yeast biomass, J. Hazard. Mater. 178 (2010) 1085–1093.
[38] L. Abramian, H. El-Rassy, Adsorption kinetics and thermodynamics of azo-dye Orange II onto highly porous titania aerogel, Chem. Eng. J. 150 (2009) 403–410.